

The Regulatory Complex of *Drosophila melanogaster* 26S Proteasomes: Subunit Composition and Localization of a Deubiquitylating Enzyme

Harald Hölzl,* Barbara Kapelari,* Josef Kellermann,* Erika Seemüller,* Máté Sümegi,† Andor Udvardy,‡ Ohad Medalia,§ Joseph Sperling,§ Shirley A. Müller,|| Andreas Engel,|| and Wolfgang Baumeister*

*Max-Planck-Institute of Biochemistry, D-82152 Martinsried, Germany; †Biological Research Center of the Hungarian Academy of Sciences, H-6701 Szeged, Hungary; §Department of Chemistry, Weizmann Institute of Science, Rehovot 76100, Israel; and ||Maurice E. Müller Institute, Biocenter, University of Basel, CH-4056 Basel, Switzerland

Abstract. *Drosophila melanogaster* embryos are a source for homogeneous and stable 26S proteasomes suitable for structural studies. For biochemical characterization, purified 26S proteasomes were resolved by two-dimensional (2D) gel electrophoresis and subunits composing the regulatory complex (RC) were identified by amino acid sequencing and immunoblotting, before corresponding cDNAs were sequenced. 17 subunits from *Drosophila* RCs were found to have homologues in the yeast and human RCs. An additional subunit, p37A, not yet described in RCs of other organisms, is a member of the ubiquitin COOH-terminal hydrolase family (UCH). Analysis of EM images of 26S

proteasomes-UCH-inhibitor complexes allowed for the first time to localize one of the RC's specific functions, deubiquitylating activity.

The masses of 26S proteasomes with either one or two attached RCs were determined by scanning transmission EM (STEM), yielding a mass of 894 kD for a single RC. This value is in good agreement with the summed masses of the 18 identified RC subunits (932 kD), indicating that the number of subunits is complete.

Key words: protein degradation • ubiquitin • ubiquitin hydrolase • ATP-dependent proteolysis • electron microscopy

Introduction

In eukaryotic cells, the vast majority of cytosolic and nuclear proteins are degraded via the ubiquitin-proteasome pathway (Rock et al., 1994). Through a sequence of activating and ligating events, ubiquitin is covalently attached to proteins destined for degradation (for recent reviews see Varshavsky, 1997; Hershko and Ciechanover, 1998; Scheffner et al., 1998). Proteins carrying multiubiquitin tags are selected by the 26S proteasome and degraded in an ATP-dependent process (Coux et al., 1996; Rechsteiner, 1998). The 26S proteasome is a large molecular machine built from ~30 different subunits that has an estimated molecular mass of 2,000–3,000 kD. Two major components jointly form the 26S (or more accurately, the 30.3S) complex: the barrel-shaped proteolytic core complex (the 20S proteasome) and the regulatory complexes (RCs),¹ which associate with either one or both ends of the

core complex (Peters et al., 1993; Yoshimura et al., 1993; see also Fig. 1).

Whereas the structure and enzymatic mechanism of the 20S proteasome have been studied in great detail (for recent reviews see Baumeister et al., 1998; Bochtler et al., 1999; Voges et al., 1999), current understanding of the structure and function of the RC is lagging behind. The RCs serve to recognize proteins carrying multiubiquitin tags and to prepare them for degradation in the 20S proteolytic complex. The preparatory steps involve the binding of the ubiquitylated substrates, their deubiquitylation, the unfolding of the substrates, and finally, their translocation into the 20S complex (Lupas et al., 1993; Rubin and Finley, 1995). Substrate unfolding is required because admission to the active site chamber inside the 20S complex is restricted to unfolded polypeptide chains (Wenzel and Baumeister, 1995). At the heart of the RCs is an array of

Address correspondence to Wolfgang Baumeister, Max-Planck-Institute of Biochemistry, Am Klopferspitz 18A, D-82152 Martinsried, Germany. Tel.: +49-89-85782642. Fax: +49-89-85782641. E-mail: baumeist@biochem.mpg.de

¹Abbreviations used in this paper: 1D, one-dimensional; 2D, two-dimensional; 16-BAC, benzyldimethyl-n-hexadecylammonium chloride; AMC, 7-amido-4-methylcoumarin; MSA, multivariate statistical analysis;

RC, regulatory complex; STEM, scanning transmission electron microscopy; Suc-LLVY-AMC, Succinyl-Leu-Leu-Val-Tyr-AMC; Ub-Al, ubiquitin COOH-terminal aldehyde; Ub-AMC, ubiquitin COOH-terminal AMC; UBP, ubiquitin-specific processing protease; UCH, ubiquitin COOH-terminal hydrolase.

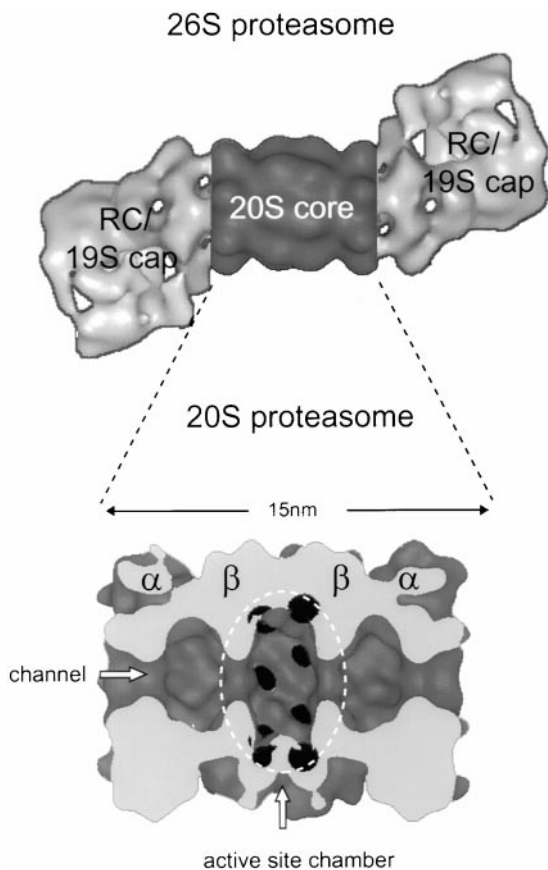


Figure 1. The 26S proteasome. The 3D model of the *Drosophila* 26S proteasome is based on EM and combined with the low-pass filtered crystal structure of the *Thermoplasma* 20S proteasome (Walz et al., 1998). The cut open side view of the 20S proteasome allows the view into the central cavity where the active sites (black) are located.

ATPases, members of the AAA family (Confalonieri and Duguet, 1995; Beyer, 1997), which act as reverse chaperones (Braun et al., 1999; Strickland et al., 2000). RCs of prokaryotic 20S proteasomes appear to have only a single type of AAA-ATPase (Wolf et al., 1998; Zwickl et al., 1999), which form homohexameric rings, whereas in eukaryotic RCs, six paralogs are found that are believed to assemble into heterohexameric rings. The hallmark of all proteasomal ATPases is an NH₂-terminal coiled-coil domain (Lupas et al., 1993; Rechsteiner, 1998). In both proteasomes and other self-compartmentalizing protein degradation machines, the proteasomes and the ATPases form colinear assemblies (Lupas et al., 1997; Zwickl et al., 2000). Thus, the ATPases are well placed to unfold substrates and control the gates that give access to the proteolytic compartments (Larsen and Finley, 1997). Beyond the ATPases, little is known about the roles of the other ~12 subunits of the RCs (for recent reviews see Tanaka and Tsurumi, 1997; Voges et al., 1999).

Structural studies with 26S proteasomes are hampered by the low stability of the complexes, which tend to dissociate into various subcomplexes. It has been shown previously that *Drosophila melanogaster* embryos provide a rich source of 26S proteasomes (Udvardy, 1993) and yield

preparations that are sufficiently homogenous for structural studies (Walz et al., 1998). To prepare the grounds for an in-depth structural analysis of the *Drosophila* RC, we sought to establish a catalog of all its subunits; to assess the completeness of this catalog, we have performed quantitative mass analysis using scanning transmission EM (STEM). In the course of these studies, we identified a novel subunit that turned out to be a deubiquitylating enzyme, p37A. Taking advantage of a nonhydrolyzable substrate analogue, ubiquitin COOH-terminal aldehyde (Ub-Al), we have been able to map its location within the complex providing new insights into the sequence of events en route to substrate degradation.

Materials and Methods

Materials

Chemicals and chromatography resins for protein purification were purchased from Sigma-Aldrich, Amersham Pharmacia Biotech, Merck, Bio-Rad, and Qiagen. Enzymes for DNA restriction and modification were obtained from New England Biolabs, Inc. and Stratagene. Oligonucleotides for PCR reactions were synthesized on an Applied Biosystems 380A DNA synthesizer.

Isolation of 26S Proteasomes from *Drosophila melanogaster* Embryos

26S proteasomes were purified as described previously (Udvardy, 1993; Walz et al., 1998). In brief, 0–16-h *Drosophila* embryos (Yellow white strain) were collected at 25°C from feeding plates. After dechorionation and homogenization, the extract was clarified by centrifugation and nucleic acids were removed by precipitation with 10% streptomycin sulfate. The supernatant was fractionated with hydroxyapatite in a batch procedure, followed by anion-exchange chromatography (diethylaminoethyl cellulose, DE52, Whatman) and sucrose density gradient centrifugation (15–40% sucrose). At all stages, fractions were tested for their ability to hydrolyze Succinyl-Leu-Leu-Val-Tyr-7-amido-4-methylcoumarin (Suc-LLVY-AMC; Bachem), and only fractions containing the peaks of activity were used for further purification. Protein concentrations were determined using the BioRad protein assay with BSA as standard.

Protein Gel Electrophoresis and Immunoblotting

SDS-PAGE was performed using 12.5% separating and 3.5% stacking gels as described by Laemmli (1970).

Protein samples were resolved by nondenaturing PAGE using a modification of the method described by Hough et al. (1987). The resolving gels were 4.6% acrylamide (37.5:1), 2.3% sucrose, 90 mM Tris, 80 mM borate, 0.08 mM EDTA, pH 8.3, polymerized with 0.04% ammonium persulfate and N,N,N',N'-tetramethyl-ethylene-diamine. The nondenaturing stacking gels contained the same buffer, but only 3.1% acrylamide (4:1). The proteins were subjected to electrophoresis in 90 mM Tris, 80 mM borate, 0.08 mM EDTA, pH 8.3, for a total of 800 V-h (50 V for 16 h) at 4°C. After electrophoresis, peptidase activity was detected by overlaying the gels with 100 μM Suc-LLVY-AMC in 5 mM MgCl₂, 10 mM KCl, 0.5 mM EDTA, 30 mM Tris, pH 7.8, for 1 h at 37°C. Proteasome bands were visualized by exposure to UV light (360 nm) and photographs were taken before staining with Coomassie blue. Alternatively, proteins were transferred to nitrocellulose membranes by semidry blotting. Blots were treated with antibodies and antigen-antibody complexes were visualized by using alkaline phosphatase-conjugated anti-mouse IgG antibodies, following standard procedures (Sambrook et al., 1989).

For two-dimensional (2D) gels, 50 μg of purified 20S or 26S proteasomes were concentrated by the use of Nanosep™ microconcentrators (Pall Filtron) and resuspended in 100 μl of loading buffer (9 M urea, 4% CHAPS, 40 mM Tris, and 0.025% Bromphenol blue). Separation in the first dimension was performed with 13-cm Immobiline® Dry Strip Gels (Amersham Pharmacia Biotech) using a linear pH gradient from 3–10. After focusing for 66,500 V-h, the strips were positioned over a vertical SDS-polyacrylamide slab gel made of a 5% stacking and 12.5% separating

gel, and subjected to electrophoresis using standard conditions. In addition the benzyltrimethyl-n-hexadecylammonium chloride (16-BAC)/SDS-PAGE, a 2D gel electrophoresis system was used as described by Hartinger et al. (1996). Proteins were either stained in the gel with Coomassie blue or electrotransferred to polyvinylidene difluoride membranes for NH₂-terminal sequencing.

Protein Sequencing

The protein-containing polyvinylidene difluoride membrane pieces were excised, cut into small pieces (3 × 3 mm), and incubated with 500 μl 0.2% polyvinylpyrrolidone (PVP 30) in water for 30 min at room temperature (Patterson, 1994). The supernatant was discarded and the membrane was washed six times with water and incubated with 0.1 M Tris-HCl, pH 8.0, 2 mM CaCl₂, 10% acetonitrile, 1% nonylphenoxy polyethoxy ethanol (Tergitol NP-40), and 0.5 μg endoproteinase LysC (Boehringer) for 8 h at 37°C. When the NH₂ terminus was blocked, protein digestion was performed in the 2D gel. Therefore, gel pieces were excised, washed twice with cleavage-buffer (12.5 mM Tris, pH 8.5, 0.5 mM EDTA, i.e., half the usual concentration), and dried. Pieces of the gel were then incubated with endoproteinase LysC for 16 h at 37°C. The resulting cleavage fragments were eluted twice with 0.1% trifluoroacetyl and once with 10% formic acid, 20% isopropanol, and 20% acetonitrile. The supernatants were dried and the peptide mixture separated on a reversed phase column Purosphere RP-18 endcapped (Merck; 1 × 150 mm). Solvent A, 0.1% trifluoroacetyl; solvent B, 0.085% trifluoroacetyl in acetonitrile. The gradient was 0–70% B over a period of 120 min at a flow rate of 60 μl/min; the detection wavelength was 206 nm. The peptides were sequenced (Edman and Begg, 1967) on a pulsed liquid phase sequencer, Procise 493 (Applied Biosystems) according to the manufacturer's instructions.

DNA Sequencing

The amino acid sequences obtained from peptide analysis were used to search the databases of the Berkeley *Drosophila* Genome Project (<http://www.fruitfly.org>) for matching DNA sequences. Five of the peptides led to genes described previously. All other peptides were homologous to distinct EST cDNA clones (Rubin et al., 2000, Table I). The longest cDNA clone of each EST clone was ordered from Genome Systems, Inc. or Research Genetics, and sequenced on both strands with a 373 DNA Sequencer using the BigDye Terminator Cycle Sequencing Ready Reaction Kit (Applied Biosystems). All sequences have been submitted to GenBank/EMBL/DBJ.

Construction and Purification of Recombinant p37A

The cDNA encoding the open reading frame for p37A was amplified by PCR, introducing an NH₂-terminal NdeI and a COOH-terminal XhoI site. The amplified DNA fragment was subcloned into the prokaryotic expression vector, pET22b, fusing a (His)₆-tag at the COOH terminus of the protein (Novagen Inc.). The construct was sequenced, confirming that no mutations had been introduced. Expression upon isopropyl-β-D-thiogalactopyranoside (Biomol) induction (1 mM, 5 h, 37°C) of *Escherichia coli* BL21 (DE3) cells (Studier et al., 1990) yielded a His-tagged protein of ~37 kD. The recombinant protein was purified on a nickel-nitrilotriacetic acid resin (Quiagen) and dialyzed against 50 mM Hepes, pH 7.8, 0.5 mM EDTA, 20% glycerol, 1 mM DTT.

Determination of Ubiquitin COOH-terminal Hydrolase Activity

Assays for p37A and 26S proteasome enzymatic activity were performed essentially as described for the ubiquitin COOH-terminal hydrolase (UCH)-L3 enzyme (Dang et al., 1998). 5 μl p37A (~1 μM) and 20 μl 26S proteasomes (~0.5 mg/ml) were incubated in 490 and 475 μl (respectively) of assay buffer (50 mM Hepes, pH 7.8, 0.5 mM EDTA, 1 mM DTT, and 0.1 mg/ml BSA) at 25°C for 1 h. The reaction was started by the addition of 5 μl of 50 μM ubiquitin COOH-terminal AMC (Ub-AMC; Affiniti) in DMSO. Reaction progress was monitored on a Perkin Elmer LS 50B luminescence spectrometer by the increase of fluorescence intensity at 460 nm (λ_{ex} = 380 nm) that accompanies cleavage of AMC from Ub-AMC. For inhibition of the 20S proteolytic activity, 10 μl of a 1 mM lactacystin (Affiniti) solution in H₂O were incubated with 20 μl 26S proteasomes in 70 μl assay buffer for 1 h at 25°C. 400 μl prewarmed assay buffer and 5 μl Ub-AMC (50 μM) were added to start the reaction. To test

Table I. Identification of the *Drosophila* RC Subunits

Spot*	Peptide sequence [†]	EST cDNA clone ID [‡]	GenBank [§]	Protein
–	VATAVLSIAARQK	LD11427		p110
–	TGETKLEKKPLL	LD05942		p97
–	TNATDIGANDVE		M63010	p58 (Dox-A2)
W	APQETYADIGGLD	}	U39303	p56 (S4)
V	GVILYGGPGTGK			
–	TGLTPVDSAA	LD07018		p55
U [¶]			S79502	p54 (S5a)
T	SEVIRITHEIQAQNEK	LD22987		p50
S	EFIEVQEEYIK	GM02119		p48A
R	FVVELADSVAP	}	LD17074	p48B
Q	QVNETGI			
O ^{**}	YLIEEGG	}	GH10329	p42A
P ^{**}				
N	EQGILQQGELQK	}	LD20236	p42B
M	XXVNREEQD			
H	VPDSTYEMYGGGLDK	}	U97538	p42C (DUG)
I	IEELQLVVAEK			
J	SLQSVGQIVGEVL		LD04678	p42D
K	HGEIDYEAIVK		LD17530	p39A
G	AIERISF			
D				
E	PSQEVSVNK	}	M64643	p39B (mov34)
F				
C	FCQCDFPYNK	LD02040		p37A
B	MTPEQCAIK	CK01641		p37B
A	IFQAK	LD13866		p30

*Proteins were resolved by 2D gel electrophoresis as shown in Fig. 2. The three largest subunits (p110, p97, and p58) were separated by 1D SDS-PAGE; p55 was identified on a 16-BAC/SDS gel.

[†]Peptides are either NH₂-terminal or internal sequences were obtained as described in Materials and Methods. X stands for unassigned residues. For all peptides, assigned residues were in complete agreement with amino acid sequences deduced from *Drosophila* genomic sequences.

[‡]Determined by a Blastp search of the *Drosophila* genome (Berkeley *Drosophila* genome project) with the shown peptide sequences.

[§]Proteins were named according to their apparent mass on 1D SDS-gels (Haracska and Udvardy, 1996). Five genes, which encode RC subunits, have been characterized previously; their original names are provided within parentheses.

[¶]Spot U was not sequenced, but identified by immunoblotting as p54.

**Spots O and P were not consistently present 2D gels and could not be sequenced. Digests of protein bands on 1D SDS gels in the molecular weight region of 42 kD revealed a peptide sequence in agreement with the *Drosophila* genomic sequence for p42A. It is assumed that one or both spots correspond to p42A.

whether the p37A activity was inhibited by Ub-A1 (BioTrend), protein samples were incubated with different concentrations of Ub-A1 before the addition of Ub-AMC.

Ubiquitin aldehyde–Colloidal Gold Conjugate

Colloidal gold particles (3.5 nm), prepared by the method of Slot and Geuze (1985), were used with minor modifications. In brief, 80 ml of 0.012% NaAuCl₄ in water and 20 ml of 0.25% tannic acid, 0.2% sodium citrate, and 1 mM potassium carbonate were heated to 60°C and rapidly mixed. The gold colloids were formed within seconds and no additional purification was needed.

Thiol groups were introduced into Ub-A1 by modifying the side chain of lysine residues. Ub-A1 (1.3 μg) and 2-iminothiolane (3 μg) in 20 μl of 50 mM triethanol amine, pH 7.3, were incubated for 6 h at room temperature. 15 μl of the thiolated Ub-A1 solution was mixed with 100 μl of freshly prepared colloidal gold solution, incubated for 8–12 h at 4°C, and centrifuged for 10 min at 80,000 g (Airfuge; Beckman Coulter). The soft pellet was resuspended in 15 μl of distilled water.

Electron Microscopy

2 μl of purified 26S proteasomes (0.2 mg/ml) was incubated with 1 μl of gold-labeled Ub-A1 and 2 μl of 20 mM Tris buffer, pH 7.2, for 7 min and applied to 100 × 400 mesh copper grids, which had been coated with carbon and glow-discharged in a plasma cleaner, for 45 s. After blotting and removing the sucrose with Tris buffer (20 mM), the preparation was nega-

tively stained with 2% aqueous uranyl acetate for 45 s. Electron micrographs were recorded digitally (Photometrix slow scan CCD; 1024 × 1024 pixels) at 45,700× using a CM12 transmission electron microscope (Philips) at 120 kV accelerating voltage.

Image Processing

The images were transferred to a SGI workstation and analyzed using the EM software package (Hegerl, 1996). Subframes containing single 26S, either with or without gold particles, were interactively extracted from the images. The two sets of complexes were separately aligned, translationally and rotationally (5 cycles), using iterative cross-correlation techniques (Baumeister et al., 1988; Phipps et al., 1991). For the set where gold labels were present, the lower cutoff of the gray level range of each frame was increased to the mean value minus $0.5 \times \text{SD}$ before alignment to minimize the contribution of the gold particles. The alignment parameters were then assigned to the original stack. Subsequently, the dataset was subjected to multivariate statistical analysis (MSA).

Scanning Transmission Electron Microscopy

For mass analysis by STEM, the 26S proteasome stock preparation (150 $\mu\text{g/ml}$) was diluted 2–8 times in buffer without sucrose, and either used directly or after cross-linking with 0.05% glutaraldehyde (final concentration) for 5 min on ice. Aliquots of the solutions were immediately adsorbed to glow-discharged thin carbon films, supported by thick perforated carbon layers on gold-coated copper grids. In the absence of cross-linking, grids were washed 4–5 times with 0.1 M ammonium acetate. The glutaraldehyde-treated samples were washed several times with quartz bi-distilled water. All grids were freeze-dried overnight in the microscope pretreatment chamber.

A Vacuum Generators STEM HB-5 interfaced to a modular computer system (Tietz Video; Image Processing Systems) and operated at 80 kV was used for the measurements. Series of 512×512 -pixel digital images were recorded at a nominal magnification of 200,000×, using doses of ~ 300 electrons/ nm^2 . The data were evaluated using the IMPSYS program package as described previously (Müller et al., 1992). To this end, the particles were classified into eight groups according to their dimensions, the selection box was kept as small as possible. Total scattering within the selection box was determined and the scattering from an equivalent area of the background support film was subtracted to calculate the particle's mass. The clearly identifiable top views of the strongly scattering 20S particles, present in all preparations, served as internal mass standards. The instrument's calibration (Müller et al., 1992) allowed the use of a single scale factor for each experiment.

The mass of the 20S particle was taken as 721 kD, i.e., the average of the calculated mass values for the yeast and human 20S proteasomes. For each experiment (two glutaraldehyde and two ammonium acetate-treated preparations), mass data from the top views were displayed in a histogram and a Gaussian curve was fitted. The position of this peak compared with 721 kD yielded a global scale factor that was subsequently applied to the whole data set. In a final step, corresponding data sets from all four experiments were pooled, displayed in histograms, and Gaussian curves were fitted. The number of complexes (n) contributing to each peak was estimated and, where relevant, the corresponding SE calculated from the SD of the Gauss curve ($\text{SE} = \text{SD}/\sqrt{n}$). After arithmetic operations, the resulting error was estimated as $\sqrt{(\sum S^2)}$ (where S is the SD or SE, respectively, of the individual results).

Results

Purification and Characterization of 26S Proteasomes from *Drosophila* Embryos

The last step of proteasome purification, the sucrose density gradient centrifugation, yielded two peaks with high peptidase activity, capable of hydrolyzing the fluorogenic peptide, Suc-LLVY-AMC. The active fractions giving rise to each peak were analyzed by SDS-PAGE (Fig. 2) and nondenaturing PAGE (Fig. 3). Fraction 10, with $\sim 22\%$ sucrose, was the first fraction of peak 1 and contained pure 20S proteasomes. Fractions 13, 14, and 15 also contained

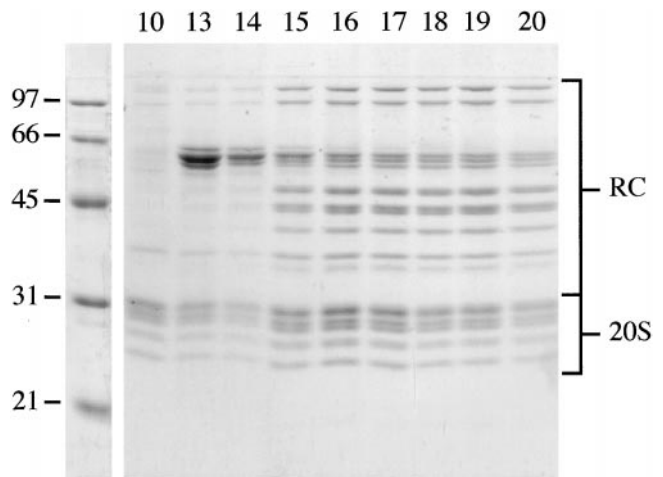


Figure 2. SDS-PAGE of 26S proteasomes. Fractions 10 and 13–20 from the sucrose density gradient centrifugation were separated on a 12.5% SDS gel and the proteins were stained with Coomassie blue. Molecular weights of the marker proteins are shown on the left. For assignment of bands see Fig. 4. Fraction 10 ($\sim 22\%$ sucrose) contained pure 20S proteasomes, and fractions 13–20 (~ 24 – 28%) displayed the typical pattern of subunit components exhibited by 26S proteasomes. Fractions 13–15 were contaminated with another protein complex (possibly a homologue of GroEL).

20S proteasomes, but these were contaminated with a high molecular weight protein that appeared similar to GroEL on electron micrographs. Fractions 16–20, from the second activity peak corresponding to ~ 26 – 28% sucrose, showed a pattern characteristic of 26S proteasomes on SDS gels. Under native conditions, the *Drosophila* complex separated into four bands, similar to the pattern observed with mammalian and yeast proteasomes (Hoffman et al., 1992; Glickman et al., 1998a). Fluorogenic peptide overlays showed, besides 20S proteasomes, two slower migrating species; for yeast proteasomes these species were identified as complete 26S proteasomes (with RCs capping both ends of the 20S proteasome, i.e., 20S-RC₂) and 26S proteasomes capped only at one end (i.e., 20S-RC₁; Glickman et al., 1998a; Fig. 3 a). The coexistence of two distinct forms of the proteasome has been shown previously by EM (Peters et al., 1993; Fujinami et al., 1994; Walz et al., 1998). To determine which bands contained the RCs, the protein complexes in fraction 19 were electroblotted from the native gels onto nitrocellulose membranes and probed with several mAbs directed against various subunits of the RC and the 20S proteasome. Fig. 3 c, lane 1, shows immunoreactivity with $\mu 3/50$, an antibody directed against the RC subunit p39A, and lane 2 shows immunoreactivity with V.D5, an antibody directed against the 20S proteasome. Several other antibodies were used to verify the assignment (data not shown). These results lead to the identification of the four resolved complexes from top to bottom as follows: 26S (20S-RC₂), single 26S (20S-RC₁), RCs, and 20S core particles, as indicated in Fig. 3.

Subunit Composition of the RC

As reported previously and illustrated by Fig. 2, *Dro-*

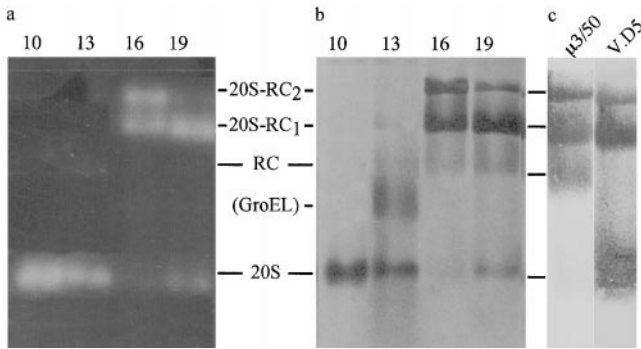


Figure 3. Nondenaturing PAGE of 26S proteasomes. Fractions 10, 13, 16, and 19 (40 μ l) from the sucrose gradients were electrophoresed for 800 V-h on 4.5% native polyacrylamide gels. a, Proteolytic activity of the resolved complexes was detected by fluorogenic peptide overlay with Suc-LLVY-AMC and the proteins were visualized by Coomassie blue stain (b; same gel). c, To further characterize the bands, duplicate samples of fraction 19 were transferred to nitrocellulose membranes and immunostained with μ 3/50, an mAb directed against the RC subunit, p39A, and with another, V.D5, directed against the 20S proteasome. The analysis of a, b, and c allowed unambiguous identification of the bands as 20S proteasomes, RCs, 26S proteasomes with only one RC attached (20S-RC₁), and 26S proteasomes with two RCs (20S-RC₂), as indicated.

Drosophila 26S proteasomes are resolved on one-dimensional (1D) gels into 12 distinct bands that are in addition to the bands that arise from the 20S core complex (Udvardy, 1993). According to their apparent mass, they are referred to as p110 to p37B (Haracska and Udvardy, 1996). A typical 2D-electrophoresis pattern of 26S proteasomes is shown in Fig. 4. The protein pattern in the 20–30-kD range closely resembles that of purified 20S proteasomes (data not shown). The proteins in the higher molecular mass range, assigned to the RC, yield >20 distinct spots with pIs between 4.8 and 8.5. These spots were analyzed further by amino acid sequencing. Since no distinct spots could be detected for the three largest subunits, p110, p97, and p58 on the 2D gels, these proteins were sequenced from a 1D SDS gel and could be unambiguously identified. Whereas p97 and p58 were directly accessible to NH₂-terminal sequencing, p110 was NH₂-terminally blocked and had to be analyzed by in-gel digestion. Of the spots on the 2D gels, only E and N were accessible for NH₂-terminal sequencing, the remaining spots were blocked due to posttranslational modifications.

All of the peptide sequences obtained were in complete agreement with the amino acid sequences deduced from the *Drosophila* genome (Table I). Only one spot above the 20–30-kD range turned out not to be an RC subunit; this protein was identified as Pros35, an α -type subunit of the 20S proteasome. Spot U was not sequenced, but clearly identified as p54 by electroblotting and probing with an mAb (μ 3/150).

On 1D SDS gels, two bands are found with apparent molecular masses close to 42 kD, corresponding to four different proteins, named p42A to p42D. The proteins p42B, p42C, and p42D were also detected on 2D gels (spots H to N). However, spots O and P, in the same mass

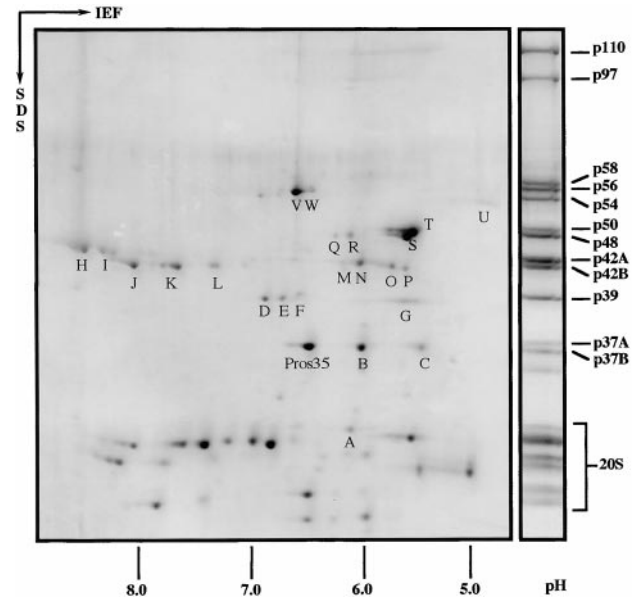


Figure 4. 2D gel electrophoresis of *Drosophila* 26S proteasomes. Purified 26S proteasomes from *Drosophila* embryos were separated in the first dimension by isoelectric focusing (IEF) with an immobilized pH gradient from 3 to 10. Next, proteins were resolved in the second dimension using a 12.5% polyacrylamide SDS gel and stained with Coomassie blue. 26S proteasomes resolved by 1D SDS-PAGE were used as molecular weight marker and the bands were named according to the procedure of Haracska and Udvardy (1996). All spots marked with a capital were identified by peptide sequencing with the exception of spot L, which could not be sequenced, and spot U, which was identified by immunoblotting (for details see Table I and Results). Low molecular weight proteins (not indicated separately) belong to the 20S core complex. With one exception, Pros35, they were not identified by peptide sequencing.

range that we assume to correspond to the fourth protein, p42A, were not always present and it was not possible to derive sequence information from them. It was also impossible to obtain sequence information for spot L, which showed very faint staining on 2D gels. Since variably migrating forms were found for several subunits (see Fig. 4 and Table I), spot L may correspond to p42D, as do spots J and K. The partially unsatisfactory resolution of the above electrophoretic system prompted the use of another gel system, 16-BAC/SDS-PAGE 2D gel electrophoresis (Hartinger et al., 1996). This gave a better separation, yielding some additional spots. Sequence comparison showed one to correspond to Rpn5/p55; no corresponding spot was found on conventional 2D gels. In the 42-kD region, no additional proteins were detected with the 16-BAC/SDS-PAGE 2D gel system.

Altogether, 18 distinct RC subunits were identified (Table II). Accordingly, the six ATPases of the AAA family (Confalonieri and Duguet, 1995; Beyer, 1997), which are integral components of all RCs investigated to date (DeMartino et al., 1994; Dubiel et al., 1995; Glickman et al., 1998a), are also present in the *Drosophila* RC. As their yeast counterparts, the six ATPases from *Drosophila* exhibit 40–50% sequence identity. The sequence identity between *Drosophila* and yeast, and between *Drosophila* and

Table II. Subunit Composition of the *Drosophila* RC

<i>Drosophila</i> RC subunits					Homologues			
Name	Accession*	AA	MW [†]	pI [‡]	Yeast [§]	Human [¶]	Identity	
					%		%	
p110	AF145303	1020	113.2	4.93	Rpn2	S1	38 (1–858)	64 (3–859)
p97	AF145304	919	102.3	5.48	Rpn1	S2	36 (65–615)	58 (65–917)
p58	M63010	494	56.0	9.04	Rpn3	S3	32 (12–458)	58 (8–494)
p56	U39303	439	49.3	6.17	Rpt2	S4	72 (24–439)	88 (1–439)
p55	AF145315	502	57.7	5.49	Rpn5	p55	38 (8–442)	47 (11–455)
p54	S79502	396	42.6	4.70	Rpn10	S5a	41 (1–225)	52 (1–381)
p50	AF145305	428	47.8	5.20	Rpt5	S6'	68 (14–428)	84 (9–428)
p48A	AF145306	412	46.9	5.22	Rpt3	S6	69 (34–413)	84 (12–413)
p48B	AF145307	433	48.5	5.75	Rpt1	S7	64 (5–433)	85 (1–433)
p42A	AF145308	389	45.4	6.06	Rpn7	S10	37 (15–389)	70 (1–389)
p42B	AF145309	422	47.3	5.66	Rpn6	S9	42 (1–421)	64 (2–422)
p42C	U97538	405	45.8	8.51	Rpt6	S8	71 (18–405)	86 (6–405)
p42D	AF145310	390	44.2	8.44	Rpt4	S10b	70 (8–388)	86 (6–390)
P39A	AF145311	382	43.8	5.18	Rpn9	S11	30 (8–379)	42 (15–381)
p39B	M64643	338	38.5	8.90	Rpn8	S12	44 (10–290)	71 (5–290)
p37A	AF145312	324	37.7	5.12		UCH37	59 (1–324)	59 (1–324)
p37B	AF145313	308	34.4	5.74	Rpn11	S13	64 (1–308)	88 (1–308)
p30	AF145314	264	30.2	5.80	Rpn12	S14	25 (25–264)	45 (7–264)

*Genbank/EMBL/DDBJ accession number.
[†]Molecular mass (kD) and pI were theoretically determined by the use of GENETYX-MAC 8.0.
[‡]Unified nomenclature for the yeast RC subunits proposed by Finley et al. (1998).
[¶]Identities were judged by Ψ-Blast searches using default parameters (<http://www.ncbi.nlm.nih.gov/blast/psiblast.cgi>). The first and last residues of the alignable regions of the *Drosophila* proteins are given in parentheses.
^{||}Except for p55 and UCH37, human RC subunits are numbered according to their SDS-PAGE mobility (Dubiel et al., 1995).

human ATPases varies between 64–72% and between 84–88%, respectively. This level of identity is much higher than that of the non-ATPases of the RC, which ranges from 25–44% and 42–71% between *Drosophila* and yeast and between *Drosophila* and human, respectively. Similar to the situation in yeast (Glickman et al., 1998a), the non-ATPase subunit, p37B, is an exception since it is 64% identical to yeast Rpn11 and 88% identical to human S13. Also, p110 (Rpn2/S1) is 25% identical to p97 (Rpn1/S2), and p39B (Rpn8/S12) is 30% identical to p37B (Rpn11/S13).

p37A, A Novel Subunit of the RC

One of the spots on the 2D gels yielded the protein sequence FCQC FDPY NK, and sequencing the corresponding EST cDNA clone, LD02040, revealed the existence of an open reading frame of 972 bp, which encodes a previously unreported protein of 324 amino acids, p37A. The predicted molecular mass of p37A, 37.672 kD, matches its mobility on SDS-PAGE gels. The predicted pI of 5.12 is slightly more acidic than that observed on 2D gels (Fig. 4). *Drosophila* p37A has no homologues among the yeast RC subunits. However, a database search revealed homologues in the human, murine, and bovine genomes, of which the human was identified as a RC subunit (Xu, W., and R.E. Cohen, personal communication). p37A is a member of the ubiquitin COOH-terminal hydrolase (UCH) family (Fig. 5; Wilkinson, 1997). UCHs form a class of thiol proteases, which remove thiols, amines, peptides, and small proteins from the COOH terminus of ubiquitin (Wilkinson, 1997). They are characterized by a 210-amino acid catalytic domain with four highly con-

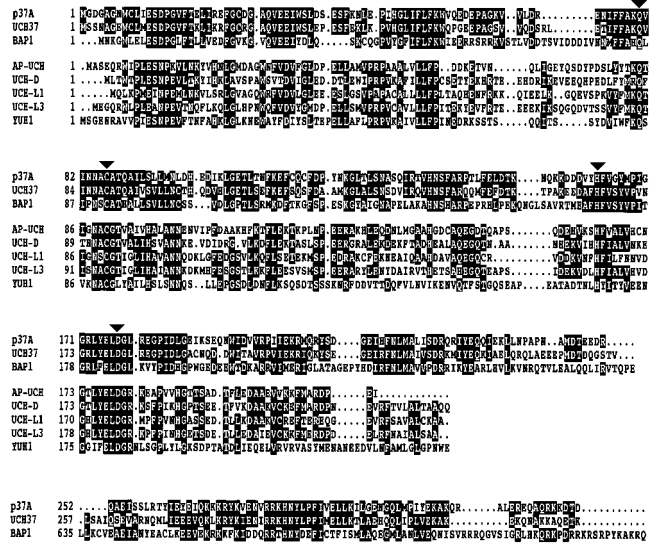


Figure 5. Sequence alignment of p37A with related UCHs. Ψ-Blast using default parameters (<http://www.ncbi.nlm.nih.gov/blast/psiblast.cgi>) was performed to search for proteins related to p37A. The identified proteins were aligned using the CLUSTAL X Multiple Sequence Alignment Program (version 1.63b; Thompson et al., 1997). UCH37 (GenBank/EMBL/DDBJ accession #A4D31528), BAP1 (GenBank/EMBL/DDBJ accession #AF045581), and p37A (GenBank/EMBL/DDBJ accession #AF145312) are more closely related to each other than to the other UCHs (AP-UCH, GenBank/EMBL/DDBJ accession #AAB52410; UCH-D, GenBank/EMBL/DDBJ accession #P35122; UCH-L1, GenBank/EMBL/DDBJ accession #P09936; UCH-L3, GenBank/EMBL/DDBJ accession #P15374; and YUH1, GenBank/EMBL/DDBJ accession #P35127). With a gap of ~400 amino acids, the COOH-terminal region of BAP1 (residues 640–716) is again homologous to p37A and UCH37. Residues conserved among p37A, UCH37, and BAP1, as well as the other five proteins are shown in reverse type. The active site residues (denoted with arrows) are conserved in all eight proteins.

served sequence blocks, containing the four active site residues. Interestingly, p37A is closely related to human BAP1 (Jensen et al., 1998). BAP1 is a nuclear protein of 81 kD, showing significant homology to the UCHs in its 240 residue NH₂-terminal domain. The COOH terminus of BAP1 is predicted to fold into a helical (possibly coiled-coil) structure, which may interact with the RING finger domain of the breast/ovarian cancer susceptibility gene product, BRCA1 (Jensen et al., 1998). Although the COOH-terminal parts of p37A (residues 252–322) and BAP1 (residues 640–716) are similar (32% identity), a coiled-coil structure for p37A is not predicted when the same algorithm (Lupas et al., 1991) is applied to the sequence.

STEM Mass Mapping

It is notoriously difficult to assess the completeness of subunit catalogs of large macromolecule assemblies by 2D electrophoresis. Therefore, it is useful to determine experimentally the mass of structurally distinct subcomplexes, such as the RC, and to compare this with the summed sequence-derived mass of their subunits. Mass mapping by

Downloaded from jcb.iupress.org on December 15, 2015

STEM (Engel et al., 1982) allows such measurements to be made with remarkable accuracy.

Images recorded for mass measurement from unstained 26S proteasome samples showed the preparations to be heterogeneous. Heterogeneity was not reduced by glutaraldehyde fixation. However, the bone-shaped side-view projections, typical of symmetrical 26S (20S-RC₂), could be clearly distinguished from the wedge-shaped projections of asymmetrical 26S (20S-RC₁) complexes. In addition, there were many ring structures with the characteristic signature of 20S proteasome particles viewed end-on, as well as less dense, almost circular projections. Since their high scattering allowed an unambiguous visual identification, the 20S proteasomes served as a convenient internal mass standard. The mass was set to 721 kD (see Materials and Methods). In this way, both slight mass differences arising from the sample preparation techniques employed, and the inherent beam-induced mass loss, could be accurately accounted for.

Pooled data sets from the four experiments were displayed in histograms and were Gaussian curve fitted (Fig. 6). The low standard deviation of ± 55 kD of the 20S proteasome particles ($n = 3,853$; SE = ± 0.9 kD; Fig. 6 b) illustrates the high quality of the calibration, yielding almost exactly the SD value expected (~ 50 kD) from background fluctuations for the small selection box size used. The mass of the wedge-shaped species, 20S-RC₁, was found to be $1,623 \pm 155$ kD ($n = 2,003$; Fig. 6 c). The mass of the 20S-RC₂ complexes was $2,508 \pm 196$ kD ($n = 286$; Fig. 6 d). The population of small particles, with lower scattering power than the 20S proteasomes' almost circular projections, had a mass of 358 ± 96 kD ($n = 1,394$; Fig. 6 a). The above data allow three estimates to be made for the mass of the RC: considering the mass of 20S-RC₂ and the mass of 20S-RC₁, mass of one RC, 885 ± 250 kD (SE = ± 12 kD); considering the mass of 20S-RC₁ and the calibration value for the 20S proteasome, mass of one RC 902 ± 164 kD (SE = ± 4 kD); and considering the mass of 20S-RC₂ and the calibration value for the 20S proteasome, mass of one RC, 894 ± 144 kD (SE = ± 8 kD). The overall average mass of the RC is 894 ± 196 kD with a SE of ± 9 kD. Although experimental data were present in this mass range, indicating the existence of some free RCs, the absence of a well defined peak on the histogram prohibited a more direct measurement of the RC mass.

This result of 894 kD correlates well with the calculated mass of the RC (932 kD), obtained by summation of the 18 individual subunits (see Table II).

Deubiquitylating Activity of p37A and the 26S Proteasome

The cDNA encoding p37A was subcloned into pET22b, after fusing a Histidine-tag to its COOH terminus, and expressed in *E. coli*. The recombinant protein could be purified under native conditions and was assayed for UCH enzymatic activity using Ub-AMC as a substrate (Dang et al., 1998). Similar to the control enzyme, UCH-L3, p37A hydrolyzed the fluorogenic substrate, and was completely inhibited by Ub-A1 when added at an equimolar concentration (Fig. 7 a). Purified 26S proteasomes were assayed in the same manner and also found to exhibit UCH enzy-

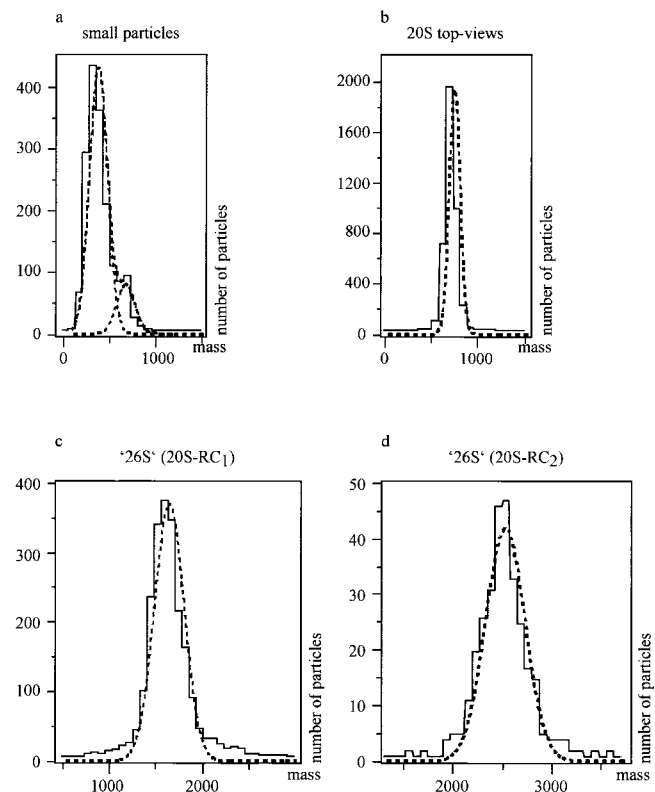


Figure 6. STEM mass measurements. Data from the four experiments performed were individually scaled to the 20S proteasome mass, 721 kD, and pooled to yield the histograms shown. a, The peaks fall at 358 ± 96 kD ($n = 1,394$; for the small particles with an almost circular projection); b, 721 ± 55 kD for the 20S proteasome top-views (internal mass standard); c, $1,623 \pm 155$ kD ($n = 2,003$) for 20S-RC₁; and d, $2,508 \pm 196$ kD ($n = 286$) for the bone-shaped 26S projections, 20S-RC₂.

matic activity (Fig. 7 b). This activity could be blocked by the addition of Ub-A1, but was not affected by the 20S proteasome inhibitor, lactacystin (Fenteany et al., 1995), which rules out the possibility that the 20S core contributes to the release of free AMC.

Mapping the Position of p37A Within the RC by Electron Microscopy

In mapping of p37A, we have taken advantage of the specific binding of the UCH inhibitor, Ub-A1. The Ub-A1 was conjugated to colloidal gold particles with a diameter of 3.5 nm. The gold particles are sufficiently electron dense to be clearly visible, even in negatively stained preparations. To obtain specific and stable conjugates, the side chain of lysine residues of Ub-A1 was extended by reacting the terminal amino group with 2-iminothiolane to give a modified side chain with a terminal primary thiol group. Stable binding to the colloidal gold particles was then achieved through a covalent gold-sulfur bond.

An electron micrograph of negatively stained 26S proteasomes, which were labeled with Ub-A1 conjugated to 3.5-nm colloidal gold particles, is shown in Fig. 8 a. About 50% of the 26S complexes have at least one bound gold particle, whereas unbound gold particles are not detected.

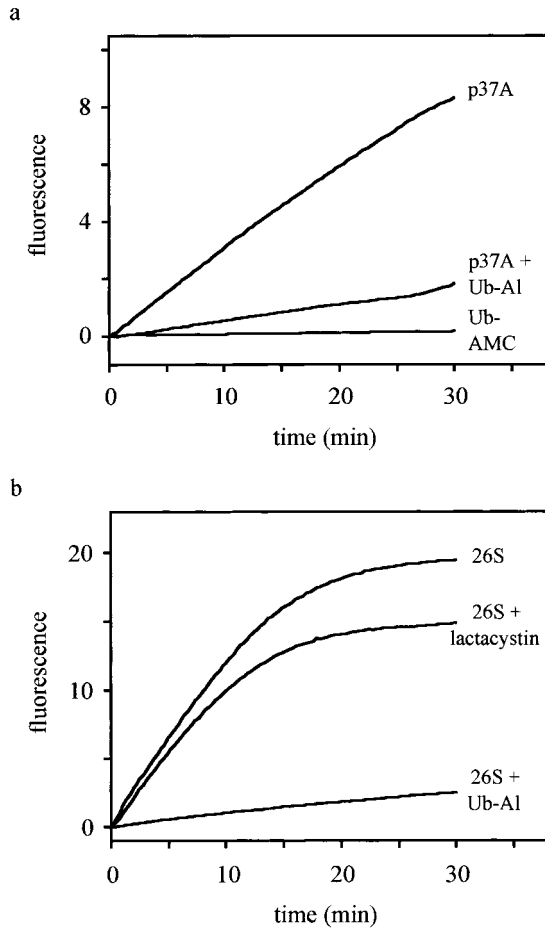


Figure 7. p37A and 26S proteasomes hydrolyze Ub-AMC. The fluorescence intensity ($\lambda_{\text{ex}} = 380 \text{ nm}$, $\lambda_{\text{em}} = 460 \text{ nm}$), which is proportional to the release of AMC, was recorded and plotted as a function of time. The reactions were performed at 25°C in assay buffer (50 mM Hepes, 0.5 mM EDTA, pH 7.8, 1 mM DTT, and 0.1 mg/ml BSA) using Ub-AMC at a final concentration of $5 \mu\text{M}$. a, The activity of p37A ($\sim 2 \text{ nM}$) was measured both with and without preincubation with Ub-AI (2 nM). In a control assay, no enzyme was added to exclude self-hydrolysis of Ub-AMC. b, Similarly, 26S proteasomes ($\sim 20 \mu\text{g/ml}$) were preincubated with and without Ub-AI (10 nM), or with lactacystin (20 μM) before addition of Ub-AMC. The difference in the levels of fluorescence between uninhibited and lactacystin-inhibited proteasomes lies within the normally observed range of deviation.

Fig. 8 b shows a gallery of aligned 26S proteasomes carrying a gold particle on either one or both sides of the complex. 2D image analysis (averages obtained after rotational and translational alignment, followed by MSA/classification) clearly map p37A to the interface between the proximal and the distal mass of the RC (Fig. 6 c), i.e., to the interface between the two RC subcomplexes, the base and the lid (Glickman et al., 1998b).

Discussion

Our understanding of the structure and function of the 26S proteasome advances at a relatively slow pace; even establishing the subunit composition is not a trivial task, given

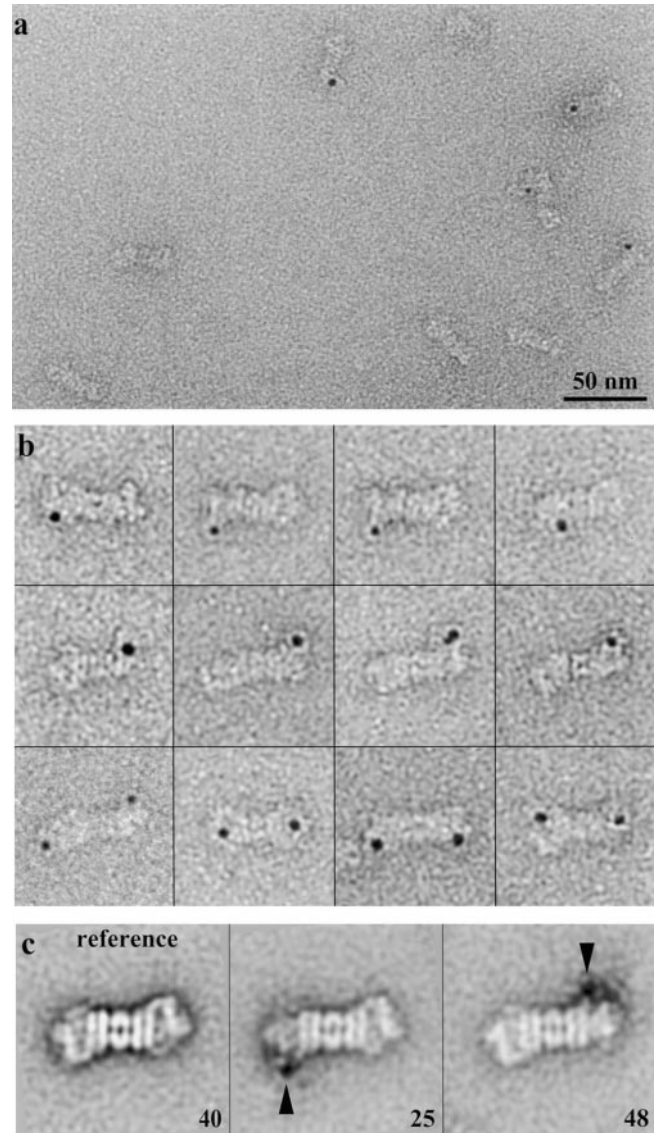


Figure 8. Mapping of p37A within the RC by EM. a, Electron micrograph of 26S proteasomes incubated with gold-labeled Ub-AI. Bar, 50 nm. b, Gallery of gold-labeled Ub-AI bound to the 26S proteasome after rotational and translational alignment. c, Main classes of unlabeled (reference) and gold-labeled 26S proteasomes after MSA/classification.

the labile nature of the complex. The bovine and human 26S complexes have been investigated in some detail and the primary structures of many of their ~ 18 electrophoretically distinct subunits in the mass range of 20–110 kD have been reported (DeMartino et al., 1994; Dubiel et al., 1995; Tanaka and Tsurumi, 1997). For yeast, a set of 18 RC subunits has been described (Glickman et al., 1998a); unfortunately, it is difficult to obtain structurally homogeneous preparations of the complex from yeast. *Drosophila* embryos have been shown to be a particularly rich source of 26S proteasomes (Udvardy, 1993), and they yield preparations that are sufficiently homogenous for structural studies (Walz et al., 1998). Initial studies with *Drosophila* RCs identified 12 subunits on 1D gels that were named

p110 to p37 (Haracska and Udvardy, 1996). However, complete primary structures have to date only been reported for p54 (Haracska and Udvardy, 1995) and p42C (DUG; Mounkes and Fuller, 1998).

To provide a platform for an in-depth structural analysis of the *Drosophila* RC, we established the subunit composition of purified 26S proteasomes by 2D gel electrophoresis and subsequent amino acid sequence analysis. In total, 18 subunits were found to constitute a single RC. 17 of them have homologues among the known yeast and mammalian RC subunits; hence, it can be assumed that none of these proteins is a contaminant and all are integral parts of the *Drosophila* RC. p37A, the only subunit missing in yeast, has homologues in mammalian 26S proteasomes (Xu, W., and R.E. Cohen, personal communication). The mammalian subunits, S5b (Deveraux et al., 1995) and p28 (Hori et al., 1998), as well as yeast Rpn4 (Fujimuro et al., 1998), have not been consistently found in 26S proteasomes from other organisms. In the *Drosophila* RC, we found no homologues of these three subunits, in agreement with their absence in *Drosophila* EST cDNA libraries.

It is hard to assert that the 18 proteins listed in Table II represent the full complement of the *Drosophila* RC subunits, as subunits may be lost during purification or escape detection on 2D gels. But the close agreement between their summed masses (932 kD) and the experimentally determined mass (894 kD) suggests that the proteins derived from 2D gels indeed represent the complete set of RC subunits from our purified 26S proteasomes. It is interesting to note that in the STEM measurements, the SDs of the mass values were somewhat larger than expected from statistical background fluctuations, with the exception of the 20S particles where the SD is very close to the theoretically expected value. This indicates that the 20S core complex is stoichiometrically well defined, while the RCs display some heterogeneity. We did not find isolated and structurally well defined particles in the range of intact RCs. Instead, we found a sizeable fraction of roughly spherical particles yielding a broad peak with a maximum at 358 kD. Probably various subcomplexes of the RC (base, lid) contribute to this slightly asymmetric peak.

Most, but not all known RC subunits have been detected in all eukaryotic organisms investigated so far; hence, there seems to be a set of constitutive proteins that are essential for functional 26S proteasomes, and in addition, facultative proteins. The latter may only be expressed in certain organisms or in a tissue-dependent manner at specific developmental stages. Some of these facultative subunits may associate only transiently with the RC, and it will depend critically on the time point when a sample is taken whether they are detected or not. In fact, transient binding to the RC has been reported for Doa4 (Papa et al., 1999) and Ap-uch (Hegde et al., 1997), and also the bona fide subunit p54 is present in free and RC-bound form (Haracska and Udvardy, 1995). Therefore, it appears unlikely that a universal number of subunits building the RC can be given.

Upon binding of ubiquitylated protein to the 26S proteasome, ubiquitin is usually recycled by means of deubiquitylating enzymes. Indeed, two different deubiquitylating activities have been reported to occur within the 26S pro-

teasome. An early study described a 30-kD ubiquitin COOH-terminal hydrolase in the RC of rabbit reticulocytes that cleaves off the remnant of target proteins from the ubiquitin chains in the course of degradation (Eytan et al., 1993). More recently, an isopeptidase activity was found that shortens ubiquitin chains conjugated to target proteins by repeated removal of distal ubiquitins (Lam et al., 1997a,b). Thus, the degradation signal of the protein is removed and poorly or erroneously ubiquitylated proteins may be rescued from proteolysis. A member of the UCH family of deubiquitylating enzymes, UCH37, is thought to be responsible for this so-called editing activity of the mammalian RC (Xu, W., and R.E. Cohen, personal communication).

We found the homologue of human UCH37 in *Drosophila* 26S proteasomes, which we named p37A, and expressed in *E. coli* for further characterization. Like other recombinant proteins of this family, it cleaves the model substrate Ub-AMC and is inhibited by Ub-Al. Thus, *Drosophila* p37A is probably different from 30-kD UCH found in proteasomes from rabbit reticulocytes, since the latter is insensitive to Ub-Al (Eytan et al., 1993). We do not know yet what type of conjugates *Drosophila* p37A prefers as substrates, but like other UCHs, it may cleave ubiquitin from peptides or small protein remnants only (Wilkinson, 1997). However, it has been shown for *Drosophila* UCH-D (Roff et al., 1996) that UCH activity may not be restricted to small leaving groups. In addition, substrate preferences may differ between the free protein and the protein integrated into the RC. Recombinant UCH37, for instance, has typical UCH specificity, i.e., it removes an intact ubiquitin chain from a ubiquitin-protein conjugate, whereas UCH37 embedded in the 19S complex shortens a ubiquitin chain from the distal end by removing ubiquitin moieties one by one, as mentioned above (Xu, W., and R.E. Cohen, personal communication).

Since we found similar enzymatic activity and inhibition profiles with native 26S proteasomes and with recombinant p37A, we assume that p37A is at least in part responsible for the deubiquitylation of proteasome-bound conjugates. The fact that no homologue exists in the yeast genome suggests that p37A is not an essential subunit of the RC, and it cannot be excluded that there are additional subunits that exhibit deubiquitylating activity. Subunit p37B is a candidate that could confer deubiquitylating activity to 26S proteasomes, since it has some sequence similarity to ubiquitin-specific processing proteases (UBP), the second family of deubiquitylating enzymes (Wilkinson, 1997). Whether p37B and its homologues, Rpn11 and S13, possess any enzymatic activity has hitherto not been shown experimentally. Since recombinant Pad1, the p37B homologue in *S. pombe*, shows no deubiquitylating activity (Penney et al., 1998), it remains questionable whether p37B and its homologues are indeed functional UBPs. Recently, it was shown that a sizeable fraction of Doa4, a 100-kD UBP, copurifies with yeast 26S proteasomes (Papa et al., 1999); however, a Doa4 homologue is not present in our preparations.

Besides p37A and UCH37, the only other UCH for which an association with 26S proteasomes has been reported is Ap-uch. Ap-uch is a neuron-specific protein, which is induced during long-term facilitation in *Aplysia*

nervous tissue and which binds transiently to 26S proteasomes (Hegde et al., 1997). We did not find an Ap-uch homologue in our preparations, but could have missed it; because of its small molecular mass, it might be difficult to separate from the 14 subunits of the 20S proteasome. Whether p37A is a constitutive component of the RC, or is only expressed during embryonic stages of the *Drosophila* development remains to be established. UCH-D, for instance, is only present in high levels during the first four hours of embryogenesis, a rapid decline to low levels follows thereafter (Zhang et al., 1993).

Although a low-resolution three-dimensional (3D) map of the *Drosophila* 26S proteasome exists (Walz et al., 1998), the mapping of specific subunits to this structural framework is only in its beginnings. There is evidence from biochemical and genetic studies that the six ATPases, all members of the AAA-ATPase superfamily, are closely associated with each other; by way of analogy to other members of the AAA-ATPase family, it has been inferred that the six paralogs form a heterohexameric ring (Voges et al., 1999). Supposing that they act as reverse chaperones, unfolding substrates before their translocation into the 20S proteolytic core, they were tentatively mapped to the interface between 20S core and the remainder of the RC (Lupas et al., 1993). Recently a combined genetic, biochemical, and structural approach has provided more definitive insights into the structural organization of the RC (Glickman et al., 1998b). In yeast, the RC has been dissected into two distinct subcomplexes, the base and the lid. The base, which is proximal to the 20S core complex, indeed comprises the six ATPases and, in addition, the two largest subunits, Rpn1 and Rpn2. The eight remaining subunits were assigned to the lid. The interaction between the base and the lid is destabilized by deletion of the subunit Rpn10. Therefore, it can be assumed that Rpn10 is critically involved in providing a structural linkage. Otherwise, the role of Rpn10 is enigmatic: it binds multiubiquitin chains in vitro (Deveraux et al., 1994), but is dispensable in vivo for the degradation of ubiquitylated proteins (Van Nocker et al., 1996). This could be reconciled if one assumes that other subunits, probably in the lid, are responsible for the initial binding of ubiquitylated proteins, while Rpn10 stabilizes the interaction further downstream in the process.

Having identified p37A as a bona fide component of the *Drosophila* RC, we have mapped its location by EM. To this end, we have taken advantage of the specific binding of the UCH inhibitor Ub-A1 to its target. By coupling Ub-A1 to 3-nm colloidal gold particles, a strong signal was generated that was clearly visible, even on unprocessed electron micrographs. On averaged images, the Ub-A1 gold conjugates map to the neck region of the dragon-head motif, i.e., the hinge between the base and the lid. This is the region where we also assume that Rpn10 is located (see above). Thus, it appears that both the binding of multiubiquitin chains and deubiquitylation are spatially closely related and perhaps also functionally coupled. One could envisage a scenario in which ubiquitylated proteins initially bind to the lid subcomplex. While being transferred to the base where the substrate is prepared for its feeding into the 20S core, Rpn10 prevents its escape while p37A recycles bound ubiquitin.

We thank M. Boicu for DNA sequencing, B. Wolpensinger for recording the STEM images, and M. Kania and D. Voges for proofreading of the manuscript.

This work was supported by the Deutsche Forschungsgemeinschaft (Bonn), Schwerpunktprogramm: "Struktur, Funktion und Regulation des 20S/26S Ubiquitin-Proteasomesystems," and the Swiss National Science Foundation.

Submitted: 2 May 2000

Revised: 30 May 2000

Accepted: 30 May 2000

References

- Baumeister, W., B. Dahlmann, R. Hegerl, F. Kopp, L. Kuehn, and G. Pfeifer. 1988. Electron microscopy and image analysis of the multicatalytic proteinase. *FEBS Lett.* 241:239-245.
- Baumeister, W., J. Walz, F. Zühl, and E. Seemüller. 1998. The proteasome: paradigm of a self-compartmentalizing protease. *Cell.* 92:3673-3680.
- Beyer, A. 1997. Sequence analysis of the AAA protein family. *Protein Sci.* 6:2043-2058.
- Bochtler, M., L. Ditzel, M. Groll, C. Hartmann, and R. Huber. 1999. The proteasome. *Annu. Rev. Biophys. Biomol. Struct.* 28:295-317.
- Braun, B.C., M. Glickman, R. Kraft, B. Dahlmann, P.M. Kloetzel, D. Finley, and M. Schmidt. 1999. The base of the proteasome regulatory particle exhibits chaperone-like activity. *Nat. Cell Biol.* 1:221-226.
- Confalonieri, F., and M. Duguet. 1995. A 200-amino acid ATPase module in search of a basic function. *Bioessays.* 17:639-650.
- Coux, O., K. Tanaka, and A.L. Goldberg. 1996. Structure and functions of the 20S and 26S proteasomes. *Annu. Rev. Biochem.* 65:801-847.
- Dang, L.C., F.D. Melandri, and R.L. Stein. 1998. Kinetic and mechanistic studies on the hydrolysis of ubiquitin C-terminal 7-amido-4-methylcoumarin by deubiquitinating enzymes. *Biochemistry.* 37:1868-1879.
- DeMartino, G.N., C.R. Moomaw, O.P. Zagnitko, R.J. Proske, M. Chu-Ping, S.J. Afendis, J.C. Swaffield, and C.A. Slaughter. 1994. PA700, an ATP-dependent activator of the 20S proteasome, is an ATPase containing multiple members of a nucleotide-binding protein family. *J. Biol. Chem.* 269:20878-20884.
- Deveraux, Q., V. Ustrell, C. Pickart, and M. Rechsteiner. 1994. A 26S protease subunit that binds ubiquitin conjugates. *J. Biol. Chem.* 269:7059-7061.
- Deveraux, Q., C. Jensen, and M. Rechsteiner. 1995. Molecular cloning and expression of a 26S protease subunit enriched in dileucine repeats. *J. Biol. Chem.* 270:23726-23729.
- Dubiel, W., G. Ferrell, and M. Rechsteiner. 1995. Subunits of the regulatory complex of the 26S proteasome. *Mol. Biol. Rep.* 21:27-34.
- Edman, P., and G.A. Begg. 1967. A protein sequenator. *Eur. J. Biochem.* 1:80-91.
- Engel, A., W. Baumeister, and W.O. Saxton. 1982. Mass mapping of a protein complex with the scanning-transmission electron-microscope. *Proc. Natl. Acad. Sci. USA* 79:4050-4054.
- Eytan, E., T. Armon, H. Heller, S. Beck, and A. Hershko. 1993. Ubiquitin C-terminal hydrolase activity associated with the 26S protease complex. *J. Biol. Chem.* 268:4668-4674.
- Fenteany, G., R.F. Standaert, W.S. Lane, S. Choi, E.J. Corey, and S.L. Schreiber. 1995. Inhibition of proteasome activities and subunit-specific amino-terminal threonine modification by lactacystin. *Science.* 268:726-731.
- Finley, D., K. Tanaka, C. Mann, H. Feldmann, M. Hochstrasser, R. Vierstra, S. Johnston, R. Hampton, J. Haber, J. Mccusker, et al. 1998. Unified nomenclature for subunits of the *Saccharomyces cerevisiae* proteasome regulatory particle. *Trends Biochem. Sci.* 23:244-245.
- Fujimuro, M., K. Tanaka, H. Yokosawa, and A. Toh-e. 1998. Son1p is a component of the 26S proteasome of the yeast *Saccharomyces cerevisiae*. *FEBS Lett.* 423:149-154.
- Fujinami, K., N. Tanahashi, K. Tanaka, A. Ichihara, Z. Cjeka, W. Baumeister, M. Miyawaki, T. Sato, and H. Nakagawa. 1994. Purification and characterization of the 26S proteasome from spinach leaves. *J. Biol. Chem.* 269:25905-25910.
- Glickman, M.H., D.M. Rubin, V.A. Fried, and D. Finley. 1998a. The regulatory particle of the *Saccharomyces cerevisiae* proteasome. *Mol. Cell. Biol.* 18:3149-3162.
- Glickman, M.H., D.M. Rubin, O. Coux, I. Wefes, G. Pfeifer, Z. Cjeka, W. Baumeister, V.A. Fried, and D. Finley. 1998b. A subcomplex of the proteasome regulatory particle required for ubiquitin-conjugate degradation and related to the COP9-signalosome and eIF3. *Cell.* 94:615-623.
- Haracska, L., and A. Udvardy. 1995. Cloning and sequencing a non-ATPase subunit of the regulatory complex of the *Drosophila* 26S protease. *Eur. J. Biochem.* 231:720-725.
- Haracska, L., and A. Udvardy. 1996. Dissection of the regulator complex of the *Drosophila* 26S protease by limited proteolysis. *Biochem. Biophys. Res. Commun.* 220:166-170.
- Hartinger, J., K. Stenius, D. Hogemann, and R. Jahn. 1996. 16-BAC/SDS-PAGE: a two-dimensional gel electrophoresis system suitable for the separation of integral membrane proteins. *Anal. Biochem.* 240:126-133.

- Hegde, A.N., K. Inokuchi, W. Pei, A. Casadio, M. Ghirardi, D.G. Chain, K.C. Martin, E.R. Kandel, and J.H. Schwartz. 1997. Ubiquitin C-terminal hydrolase is an immediate-early gene essential for long-term facilitation in *Aplysia*. *Cell* 89:115–126.
- Hegerl, R. 1996. The EM program package: a platform for image processing in biological electron microscopy. *J. Struct. Biol.* 116:30–34.
- Hershko, A., and A. Ciechanover. 1998. The ubiquitin system. *Annu. Rev. Biochem.* 67:425–479.
- Hoffman, L., G. Pratt, and M. Rechsteiner. 1992. Multiple forms of the 20S multicatalytic and the 26S ubiquitin/ATP-dependent proteases from rabbit reticulocyte lysate. *J. Biol. Chem.* 267:22362–22368.
- Hori, T., S. Kato, M. Saeki, G.N. DeMartino, C.A. Slaughter, J. Takeuchi, A. Toh-e, and K. Tanaka. 1998. cDNA cloning and functional analysis of p28 (Nas6p) and p40.5 (Nas7p), two novel regulatory subunits of the 26S proteasome. *Gene* 216:113–122.
- Hough, R., G. Pratt, and M. Rechsteiner. 1987. Purification of two high molecular weight proteases from rabbit reticulocyte lysate. *J. Biol. Chem.* 262:8303–8313.
- Jensen, D.E., M. Proctor, S.T. Marquis, H.P. Gardner, S.I. Ha, L.A. Chodosh, A.M. Ishov, N. Tommerup, H. Vissing, Y. Sekido, et al. 1998. BAP1: a novel ubiquitin hydrolase which binds to the BRCA1 ring finger and enhances BRCA1-mediated cell-growth suppression. *Oncogene* 16:1097–1112.
- Laemmli, U.K. 1970. Cleavage of structural proteins during assembly of the head of bacteriophage T4. *Nature* 227:680–683.
- Lam, Y.A., G.N. DeMartino, C.M. Pickart, and R.E. Cohen. 1997a. Specificity of the ubiquitin isopeptidase in the PA700 regulatory complex of 26S proteasomes. *J. Biol. Chem.* 272:28438–28446.
- Lam, Y.A., W. Xu, G.N. DeMartino, and R.E. Cohen. 1997b. Editing of ubiquitin conjugates by an isopeptidase in the 26S proteasome. *Nature* 385:737–740.
- Larsen, C.N., and D. Finley. 1997. Protein translocation channels in the proteasome and other proteases. *Cell* 91:431–434.
- Lupas, A., M. Van Dyke, and J. Stock. 1991. Predicting coiled coils from protein sequences. *Science* 252:1162–1164.
- Lupas, A., A.J. Koster, and W. Baumeister. 1993. Structural features of 26S and 20S proteasomes. *Enz. Prot.* 47:252–273.
- Lupas, A., J.M. Flanagan, T. Tamura, and W. Baumeister. 1997. Self-compartmentalizing proteases. *Trends Biochem. Sci.* 22:399–404.
- Mounkes, L.C., and M.T. Fuller. 1998. The *DUG* gene of *Drosophila melanogaster* encodes a structural and functional homolog of the *Saccharomyces cerevisiae* *SUG1* predicted ATPase associated with the 26S proteasome. *Gene* 206:165–174.
- Müller, S.A., N.G. Kenneth, R. Bürki, R. Häring, and A. Engel. 1992. Factors influencing the precision of quantitative scanning transmission electron microscopy. *Ultramicroscopy* 46:317–334.
- Papa, F.R., A.Y. Amerik, and M. Hochstrasser. 1999. Interaction of the Doa4 deubiquitinating enzyme with the yeast 26S proteasome. *Mol. Biol. Cell* 10:741–756.
- Patterson, S.D. 1994. From electrophoretically separated protein to identification: strategies for sequence and mass analysis. *Anal. Biochem.* 221:1–15.
- Penney, M., C. Wilkinson, M. Wallace, J.P. Javerzat, K. Ferrell, M. Seeger, W. Dubiel, S. McKay, R. Allshire, and C. Gordon. 1998. The *pad1(+)* gene encodes a subunit of the 26S proteasome in fission yeast. *J. Biol. Chem.* 273:23938–23945.
- Peters, J.M., Z. Cejka, J.R. Harris, J.A. Kleinschmidt, and W. Baumeister. 1993. Structural features of the 26S proteasome complex. *J. Mol. Biol.* 234:932–937.
- Phipps, B.M., A. Hoffmann, K.O. Stetter, and W. Baumeister. 1991. A novel ATPase complex selectively accumulated upon heat shock is a major cellular component of thermophilic archaeobacteria. *EMBO (Eur. Mol. Biol. Organ.) J.* 10:1711–1722.
- Rechsteiner, M. 1998. The 26S proteasome. In *Ubiquitin and the Biology of the Cell*. J.M. Peters, J.R. Harris, and D. Finley, editors. Plenum Press, New York. 147–189.
- Rock, K.L., C. Gramm, L. Rothstein, K. Clark, R. Stein, L. Dick, D. Hwang, and A.L. Goldberg. 1994. Inhibitors of the proteasome block the degradation of most cell proteins and the generation of peptides presented on MHC class I molecules. *Cell* 78:761–771.
- Roff, M., J. Thompson, M.S. Rodriguez, J.M. Jacque, F. Baleux, F. Arenzana-Seisdedos, and R.T. Hay. 1996. Role of I κ B α ubiquitination in signal-induced activation of NF κ B *in vivo*. *J. Biol. Chem.* 271:7844–7850.
- Rubin, D.M., and D. Finley. 1995. The proteasome: a protein-degrading organelle? *Curr. Biol.* 5:854–858.
- Rubin, G.M., L. Hong, P. Brokstein, M. Evans-Holm, E. Frise, M. Stapleton, and D.A. Harvey. 2000. A *Drosophila* complementary DNA resource. *Science* 287:2222–2224.
- Sambrook, J., E.F. Fritsch, and T. Maniatis. 1989. *Molecular Cloning: a Laboratory Manual*. 2nd edition. Cold Spring Harbor Laboratory Press, Cold Spring Harbor, NY.
- Scheffner, M., S. Smith, and S. Jentsch. 1998. The ubiquitin-conjugation system. In *Ubiquitin and the Biology of the Cell*. J.M. Peters, J.R. Harris, and D. Finley, editors. Plenum Press, NY. 65–98.
- Slot, J.W., and H.J. Geuze. 1985. A new method of preparing gold probes for multiple-labeling cytochemistry. *Eur. J. Cell Biol.* 38:87–93.
- Strickland, E., K. Hakala, P.J. Thomas, and G.N. DeMartino. 2000. Recognition of misfolding proteins by PA700, the regulatory subcomplex of the 26S proteasome. *J. Biol. Chem.* 275:5565–5572.
- Studier, F.W., A.H. Rosenberg, J.J. Dunn, and J.W. Dubendorf. 1990. Use of T7 RNA polymerase to direct expression of cloned genes. *Methods Enzymol.* 185:60–89.
- Tanaka, K., and C. Tsurumi. 1997. The 26S proteasome: subunits and functions. *Mol. Biol. Rep.* 24:3–11.
- Thompson, J.D., T.J. Gibson, F. Plewniak, F. Jeanmougin, and D.G. Higgins. 1997. The ClustalX windows interface: flexible strategies for multiple sequence alignment aided by quality analysis tools. *Nucl. Acids Res.* 25:4876–4882.
- Udvardy, A. 1993. Purification and characterization of a multiprotein component of the *Drosophila* 26S (1500 kD) proteolytic complex. *J. Biol. Chem.* 268:9055–9062.
- Van Nocker, S., S. Sadis, D.M. Rubin, M. Glickman, H. Fu, O. Coux, I. Wefes, D. Finley, and R.D. Vierstra. 1996. The multiubiquitin-chain-binding protein Mcb1 is a component of the 26S proteasome in *Saccharomyces cerevisiae* and plays a nonessential, substrate-specific role in protein turnover. *Mol. Cell Biol.* 16:6020–6028.
- Varshavsky, A. 1997. The ubiquitin system. *Trends Biochem. Sci.* 22:383–387.
- Voges, D., P. Zwickl, and W. Baumeister. 1999. The 26S proteasome: a molecular machine designed for controlled proteolysis. *Annu. Rev. Biochem.* 68:1015–1068.
- Walz, J., A. Erdmann, M. Kania, D. Typke, A.J. Koster, and W. Baumeister. 1998. 26S proteasome structure revealed by 3-dimensional electron microscopy. *J. Struct. Biol.* 121:19–29.
- Wenzel, T., and W. Baumeister. 1995. Conformational constraints in protein degradation by the 20S proteasome. *J. Struct. Biol.* 2:199–204.
- Wilkinson, K.D. 1997. Regulation of ubiquitin-dependent processes by deubiquitinating enzymes. *FASEB J.* 11:1245–1256.
- Wolf, S., I. Nagy, A. Lupas, G. Pfeifer, Z. Cejka, S.A. Müller, A. Engel, R. De Mot, and W. Baumeister. 1998. Characterization of ARC, a divergent member of the AAA ATPase family from *Rhodococcus erythropolis*. *J. Mol. Biol.* 277:13–25.
- Yoshimura, T., K. Kameyama, T. Takagi, A. Ikai, F. Tokunaga, T. Koide, N. Tanahashi, T. Tamura, Z. Cejka, W. Baumeister, et al. 1993. Molecular characterization of the 26S proteasome complex from rat liver. *J. Struct. Biol.* 111:200–211.
- Zhang, N., K.D. Wilkinson, and M. Bownes. 1993. Cloning and analysis of expression of a ubiquitin carboxyl terminal hydrolase expressed during oogenesis in *Drosophila melanogaster*. *Dev. Biol.* 157:214–223.
- Zwickl, P., D. Nig, K. Min Woo, H.P. Klenk, and A.L. Goldberg. 1999. An archaeobacterial ATPase, homologous to ATPases in the eukaryotic 26S proteasome, activates protein breakdown by 20S proteasomes. *J. Biol. Chem.* 274:26008–26014.
- Zwickl, P., W. Baumeister, and A. Steven. 2000. Dis-assembly lines: the proteasome and related ATPase-assisted proteases. *Curr. Opin. Struct. Biol.* 10:242–250.